Eco-Environment & Health 3 (2024) 317–324

Contents lists available at ScienceDirect

Eco-Environment & Health

journal homepage: www.journals.elsevier.com/eco-environment-and-health

Original Research Article

Effects of transient flow conditions on colloid-facilitated release of decabromodiphenyl ether: Implications for contaminant mobility at e-waste recycling sites

Yueyue Li [1], Zebin Huo [1], Yuqin Ying, Lin Duan, Chuanjia Jiang [*], Wei Chen

College of Environmental Science and Engineering, Ministry of Education Key Laboratory of Pollution Processes and Environmental Criteria, Tianjin Key Laboratory of Environmental Remediation and Pollution Control, Nankai University, Tianjin 300350, China

ARTICLE INFO

Keywords:
Hydrophobic organic contaminants
Colloid-facilitated transport
Dry–wet cycle
Freeze–thaw cycle
Undisturbed soil core

ABSTRACT

Polybrominated diphenyl ethers (PBDEs) are ubiquitous contaminants, especially in the soil and groundwater of contaminated sites and landfills. Notably, 2,2′,3,3′,4,4′,5,5′,6,6′-decabromodiphenyl ether (BDE-209), one of the most frequently and abundantly detected PBDE congeners in the environment, has recently been designated as a new pollutant subject to rigorous control in China. Colloid-facilitated transport is a key mechanism for the release of PBDEs from surface soils and their migration in the aquifer, but the effects of hydrodynamic conditions, particularly transient flow, on colloid-facilitated release of PBDEs are not well understood. Herein, we examined the effects of typical transient flow conditions on the release characteristics of colloids and BDE-209 from surface soil collected from an e-waste recycling site by undisturbed soil core leaching tests involving multiple dry–wet cycles (with different drying durations) and freeze–thaw cycles. We observed significant positive correlations between BDE-209 and colloid concentrations in the leachate in both the dry–wet and freeze–thaw leaching experiments, highlighting the critical role of colloids in facilitating BDE-209 release. However, colloids mobilized during the dry–wet cycles contained higher contents of BDE-209 than those in the freeze–thaw cycle tests, and the difference was primarily due to the more intensive disintegration of soil aggregates and elution of newly formed inorganic colloidal particles (mainly primary silicate minerals such as quartz and albite) with low BDE-209 content during the freeze–thaw process. These findings underscore the necessity of considering transient flow conditions when assessing the fate and risks of PBDEs at contaminated sites.

1. Introduction

Polybrominated diphenyl ethers (PBDEs) are widely used flame retardants in industries and consumer products, e.g., electronics, textiles, and plastics [1]. Due to their toxicities and persistence [2,3], the environmental fate and risks of PBDEs have raised concerns globally [4–6]. Three technical PBDE mixtures, including commercial pentaBDE (mainly tetrabromodiphenyl ethers and pentabromodiphenyl ethers), commercial octaBDE (mainly hexabromodiphenyl ethers and heptabromodiphenyl ethers), and commercial decaBDE (mainly 2,2′,3,3′,4,4′,5,5′,6,6′-decabromodiphenyl ether [BDE-209] and nonabromodiphenyl ethers), have been included in Annex A of the Stockholm Convention as persistent organic pollutants (POPs) [7–9]. Notably, BDE-209 is one of the most frequently detected and abundant PBDE congeners in the environment [10,11]. For example, high concentrations of BDE-209 were reported in soil [12–17], freshwater and marine sediments [16–20], and indoor dusts [21–23] in China. BDE-209 has been banned in many regions of the world, including many countries in Europe and North America [24,25], and recently, it has been designated as a key new pollutant subject to rigorous control in China [26]. PBDEs have been detected worldwide [27,28], with high contamination levels detected in the surface soils of electronic waste (e-waste) recycling sites [29,30] and some landfills [31]. Although PBDEs exhibit strong hydrophobicity and low solubility in water, their congeners have been reported to leach from surface soils into aquifers [32], leading to the contamination of groundwater [33–35]. Soil colloidal particles, characterized by their relatively high mobility in porous media and

* Corresponding author.
E-mail address: jiangcj@nankai.edu.cn (C. Jiang).
[1] These authors contributed equally to this work.

https://doi.org/10.1016/j.eehl.2024.03.002
Received 14 December 2023; Received in revised form 7 March 2024; Accepted 7 March 2024
Available online 26 March 2024

affinities for various environmental pollutants, can serve as vectors for the transport of contaminants in the subsurface. Consequently, colloid-facilitated transport is a major mechanism for the release of hydrophobic organic pollutants, including PBDEs, from surface soils and their migration in groundwater [36–39].

The extent of colloid-facilitated transport of PBDEs depends on the physicochemical properties of the soil colloids as well as the solution composition and hydrodynamic conditions of the aquifer. It has been reported that the capability of soil colloids to enrich PBDEs depends on the properties of soil, such as the presence of soil organic matter [40,41]. Moreover, according to leaching experiments with undisturbed soil cores collected from an e-waste recycling site (hereafter referred to as e-waste site), the ionic strength of infiltration water can significantly affect the release of colloids and BDE-209 from the surface soil [38]. Besides these factors, hydrodynamic conditions can significantly shape the transport behavior of colloids in porous media, especially in the shallow vadose zone [42–45]. Compared to steady infiltration, transient flow conditions, typically related to rainfall, snowmelt [46], and accidental discharge of wastewater can affect the soil moisture content and the flow rate of soil water, leading to an increased release of colloids [47–51]. During dry–wet cycles, the drying period preceding rainfall can influence colloid release during transient infiltration by affecting the moisture content and capillary pressure of soil [48,52], but prolonged drying can diminish colloid release by reinforcing the soil aggregate structure [52] or hydraulically disconnecting previously saturated pores from the main leaching pathway [48]. Besides the dry–wet process, the freeze–thaw process of soil porewater due to seasonal and even diurnal temperature changes [53], which usually accompanies snowfall and snowmelt, may have additional effects on the release of soil colloids and contaminants. During freezing, the expansive phase transition of liquid water into ice exerts pressure on pore walls, disintegrating soil aggregates and promoting colloid formation and release into pore water during the thaw process [50]. Considering the critical roles of soil colloids in mobilizing PBDEs in the subsurface, it can be hypothesized that transient flow significantly affects the release of colloids as well as PBDEs from surface soil to the aquifer. Understanding the influences of typical transient flow conditions on the colloid-facilitated release of PBDEs is crucial for accurately forecasting the fate and risks of these hydrophobic contaminants at contaminated sites.

Here, we aimed to examine the effects of typical transient flow conditions on the release characteristics of colloids and BDE-209 from surface soil. Leaching tests involving multiple dry–wet cycles (with different drying durations) and freeze–thaw cycles were performed using undisturbed soil cores collected from an e-waste site in Taizhou, China. Our observations revealed significant positive correlations between BDE-209 and colloid concentrations in the leachate during both the dry–wet and freeze–thaw leaching tests, highlighting the critical role of colloids in facilitating BDE-209 release. Furthermore, we found that colloids mobilized in the dry–wet cycles contained higher contents of BDE-209 than those in the freeze–thaw cycles, and the difference is primarily due to the more intensive disintegration of soil aggregates and elution of newly formed inorganic colloidal particles with low BDE-209 content during the freeze–thaw process. These findings underscore the necessity of considering transient flow conditions when assessing the fate and risks of PBDEs at contaminated sites and can aid in the design of hydrological intervention measures to curtail the spreading of hydrophobic POPs into sensitive subsurface environments.

2. Materials and methods

2.1. Materials

Undisturbed soil cores were collected from an e-waste site (28°31′59.36″N, 121°21′49.42″E) in Taizhou, Zhejiang Province, China. The once-active e-waste-dismantling practices at the site had already ceased before the soil core sampling was performed, but the soil was laden with relatively high levels of PBDEs, predominantly BDE-209 (Table S1).

Before extracting the cores, the plants were carefully removed without damaging the topsoil layer. Using a stainless-steel sampler (7.5-cm diameter) designed specifically for a core holder, soil cores from the top 0- to 10-cm layer were collected. Both the sampler and the soil core within were immediately sealed to preserve their original condition. They were then transported to the laboratory and were stored at a temperature of 4 °C for use.

Information on the chemicals and reagents used in the study is provided in Supplementary Material (SM).

2.2. Experimental apparatus

The leaching apparatus (Fig. S1) for the undisturbed soil core leaching test was the same as that used in our previous study [38]. The soil core, together with the sampler, was placed into a core holder for the leaching test. Notably, the base of the core holder was designed with seven effluent ports, each covering a water flow collection area of 2.0 cm^2. Simulated infiltration water (with the preparation method given in SM and Table S2) was pumped into the soil core with a designated flow rate of 1.5 cm/h (Darcy velocity).

2.3. Experimental procedure

2.3.1. Dry–wet cycle tests

Prior to the dry–wet cycles, the undisturbed soil core was pre-leached with a simulated infiltration solution (at 0.01-mM ionic strength and pH of 4.4) at a consistent flow rate of 1.5 cm/h for 24 h. This preliminary step was designed to stabilize the moisture content in the soil core and flush out soluble contaminants. Following this step, the leaching was stopped, allowing the core to drain naturally under gravitational force [54]. After 0.7 d of drying, the soil core underwent a 48-h leaching phase at the same flow rate using the aforementioned simulated infiltration. During this phase, effluents were collected from the ports into glass tubes at 12-h intervals for subsequent analyses. This process was repeated, and the soil core experienced five additional dry–wet cycles with varying drying durations (1.5, 2.5, 3.4, 4.6, and 8.8 days) [48].

2.3.2. Freeze–thaw cycle tests

A different soil core was used in the freeze–thaw cycle tests. Prior to the freeze–thaw cycles, the core was pre-leached and gravitationally drained using the same procedure as that described in *Section 2.3.1*. The core was then subjected to a freezing regime at −20 °C for 48 h, followed by a thawing period lasting 24 h under ambient conditions. Subsequent to the thawing, leaching resumed using the same simulated infiltration at 1.5 cm/h for 48 h. During this leaching phase, effluent samples were acquired at 12-h intervals for analyses. This entire procedure was then repeated, with the soil core undergoing four additional freeze–thaw cycles.

2.4. Analyses of leachates

Effluent samples from active ports were analyzed for the concentration, hydrodynamic diameter (D_h), ζ-potential, mineral composition, and morphology of colloids, as well as the concentration of BDE-209.

The concentration of colloids (mg/L) in the effluent samples was measured using an ultraviolet-visible spectrophotometer (G9821A, Agilent Technologies, USA) [44], with more information given in SM. The D_h and ζ-potential of colloids in the effluent were measured by using a Litesizer 500 instrument (Anton Paar). The mineral composition and morphology of the colloids in the effluent were characterized using an X-ray diffraction (XRD) instrument (Ultima IV, Rigaku, Japan) and a transmission electron microscope (TEM) (JEM-2800, JOEL, Japan). The

concentrations of common metals (Al, Fe, Ca, Mg, K, Mn, and Na) in the surface soil and colloids were determined using inductively coupled plasma optical emission spectroscopy (Agilent 730, USA) after microwave digestion. The composition of organic substances in the effluent was qualitatively determined by excitation emission matrix (EEM) fluorescence spectroscopy. More detailed characterization methods are provided in SM.

Following liquid–liquid extraction (see SM for details) [55], BDE-209 concentration was determined on an Agilent 6890N gas chromatograph (GC) with an electron capture detector (ECD) (details given in SM). Moreover, the concentrations of 14 PBDE congeners in the surface soil (Table S1) were determined by gas chromatography–mass spectrometry (GC–MS) (7890A-5975C, Agilent Technology, USA) after Soxhlet extraction [41], with detailed methods provided in SM. Initial evaluations with GC–MS revealed that, among the 14 PBDE congeners present in the soil, only BDE-209 was detectable in the effluent. Therefore, a BDE-209 standard solution was used for the GC–ECD analysis.

Additionally, the pH and conductivity of the effluent were measured using a pH meter (model S210-B) and a conductivity meter (model FE30), both manufactured by Mettler Toledo, USA.

2.5. Quality assurance/quality control

Data with a signal-to-noise ratio exceeding a value of 3 were used for further analysis. The calibration curves yielded correlation coefficients > 0.994. For BDE-209, the method detection limit (MDL) stood at 0.07 ng/L. The recovery ratios for the surrogate standard, BDE-77, spanned between 67% and 106%. Due to the narrow range observed in surrogate standard recovery, the PBDE concentrations were not adjusted based on surrogate recovery. The recovery ratios of BDE-209 in spiked blanks (BDE-209 dissolved in simulated infiltration water, which underwent the same extraction and analysis procedures as the effluent samples) ranged from 77% to 102%.

2.6. Statistical analysis

Statistical analysis was performed using SPSS version 26.0 (IBM, USA). Pearson correlation analysis and linear fitting were performed for the concentrations of colloids and BDE-209.

3. Results and discussion

3.1. Effect of dry–wet cycles on the release of colloids and BDE-209

During the leaching test with different drying durations, we observed distinct preferential flow pathways in the soil core (Fig. 1 and Table S3): water primarily eluted from two of the seven ports, and no leachate was collected from the other five ports (denoted as No. 1 and 2). The water flux from each port was relatively constant during the tests, both exceeding the application rate of the simulated infiltration (i.e., 1.5 cm/h). Notably, port No. 2 was the primary drainage port, with a flux two or three times higher than that of port No. 1. These preferential flow paths could substantially enhance the release and downward migration of colloids and the adsorbed contaminants [48,50,54].

The duration of the drying period played a pivotal role in colloid release. As the drying time increased to 2.5 or 3.4 d, an increase in colloid concentration in the leachate was observed; when the drying time further increased, colloid concentration decreased (Fig. 1 and Table S3). The colloid mass eluted from the soil core for different drying durations also followed this trend (Fig. 2), which has been noted in dry–wet leaching experiments by Majdalani et al. [52] and Mohanty et al. [48]. The increase in colloid release with longer drying time below the critical drying duration (CDD) could be attributed to the fact that the drying process can induce differential capillary stress within soil pores, resulting in colloid generation through the cracking of soil pore walls [48,56–58]. Since soil fractures are commonly coated with iron and manganese oxyhydroxides [48,59], higher concentrations of Fe and Mn are expected in the leached colloids than in bulk soil [48]. In this study, the concentrations of Fe and Mn in colloids were 1.41 and 1.37 times that in bulk soil, respectively (Fig. S2), corroborating the hypothesis that dry–wet cycles can generate colloids through the cracking of soil pore walls. However, beyond the CDD, a reduction in colloid release with longer drying time could result from hydraulic disconnection of micropores within the soil matrix from the preferential flow paths (mainly macropores and fractures) after prolonged drying, leading to diminished migratory potential of colloids from the soil matrix [48]. Furthermore, prolonged drying may result in the deposition of minerals and salts, impeding colloid mobilization [48,52,60]. It is noted that the CDD observed in this study (i.e., 2.5–3.4 d) was similar to that reported by Mohanty et al. [48] but was shorter than that (9–11 d) reported by Majdalani et al. [52], likely due to differences in the properties of the soil cores used in the studies. Specifically, the soil cores used in our study and by Mohanty et al. [48] contained abundant macropores or cracks, and the higher water permeability and abundance of preferential flow paths allowed for swifter drainage of water. Conversely, the soil used by Majdalani et al. [52] lacked macropores or cracks, leading to a longer duration for the drying front to reach the soil matrix. Moreover, the low-flux port No. 1 exhibited a CDD (3.4 d) longer than that for the high-flux port No. 2 (2.5 d), further corroborating the dependence of the CDD on the water permeability of the soil.

With the varying drying duration, the average D_h of colloids in the effluent remained relatively stable, ranging from 428 ± 25 nm to 508 ± 50 nm (Fig. 1 and Table S3). However, the ζ-potential was more negative for the drying durations of 2.5 and 3.4 d (Fig. 1 and Table S3), when relatively high colloid concentrations were observed. The similar trends between the ζ-potential and concentration of eluted colloids may be ascribed to the role of electrostatic repulsion in colloid mobilization: when the dried soil is saturated with infiltrating water, the soil colloid particles that bear more negative ζ-potential experience stronger electrostatic repulsion from the soil matrix, making it more likely for these particles to detach from soil pore walls and migrate with the infiltrating water.

The drying duration had a limited effect on the conductivity or pH of the effluent. However, during each dry–wet cycle, the conductivity in the initial leaching stage (i.e., by the first 12 h) was much higher than that in subsequent stages. This trend was due to the deposition of soluble salts on the surface of soil pore walls during drying, and the accumulated salts quickly dissolved upon the onset of leaching, resulting in the initial high conductivity (ranging from 252.0 to 381.0 μS/cm, on average 331.8 ± 29.5 μS/cm). As leaching proceeded, the salts accumulated on the pore walls were depleted, and the conductivity of the effluent depended on the content of ions in the soil matrix exchangeable with the infiltrate, which was relatively stable for a given soil core. By the end of the leaching in each dry–wet cycle, the conductivity was in the narrow range of 70.3–96.0 μS/cm, with an average of 83.9 ± 7.9 μS/cm. Regardless of the drying duration, the pH of the effluent was consistently between 7.4 and 7.8, though the pH of the influent was 4.4. The insensitivity of effluent pH to influent pH during soil core leaching tests has been previously observed and ascribed to the pH buffering capacity of soil [38].

During the dry–wet leaching experiments, BDE-209 concentration in the effluent samples from port No. 2 was in the range from 0.09 to 0.48 ng/L (Table S3). However, BDE-209 was not detected in the effluent from port No. 1, which was attributed to the low colloid mass in the leachate from port No. 1, rendering the BDE-209 mass in the analytical sample below detection. The average BDE-209 concentration during the dry–wet leaching experiments was 0.21 ± 0.15 ng/L (Table 1), which was lower than that in the effluent from soil cores collected from an e-waste site in Tianjin, despite comparable colloid concentrations in the effluents [38]. This difference is likely due to the much higher BDE-209 content in soil at the site in Tianjin [41].

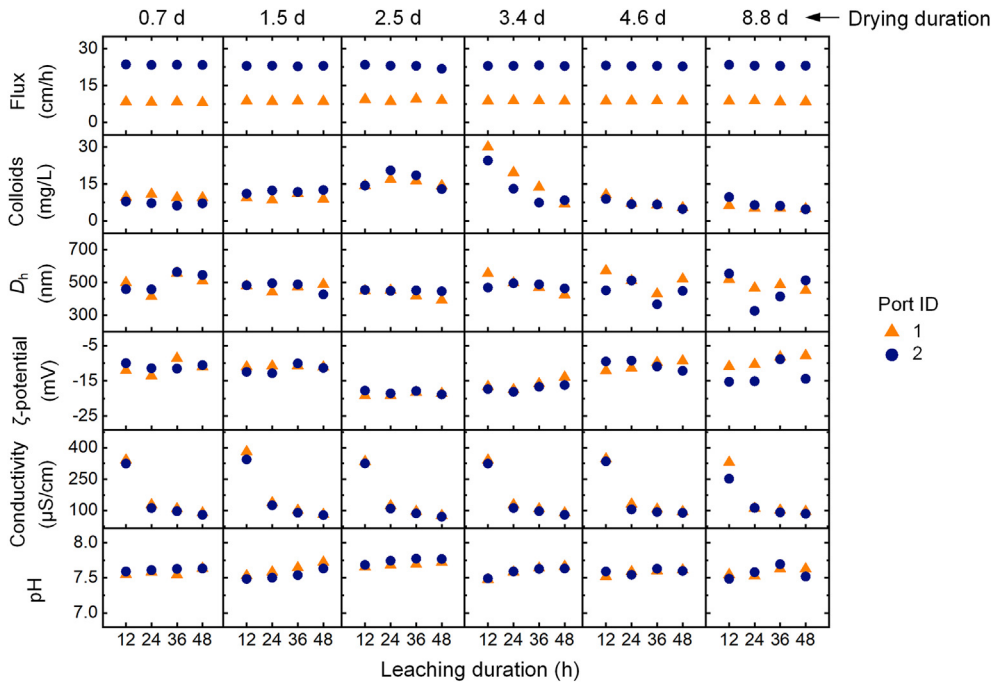

Fig. 1. Effluent flux, colloid concentration, D_h, ζ-potential, conductivity, and pH from two active ports during dry–wet cycle tests at different drying durations. Influent Darcy velocity = 1.5 cm/h, ionic strength = 0.01 mM, pH = 4.4.

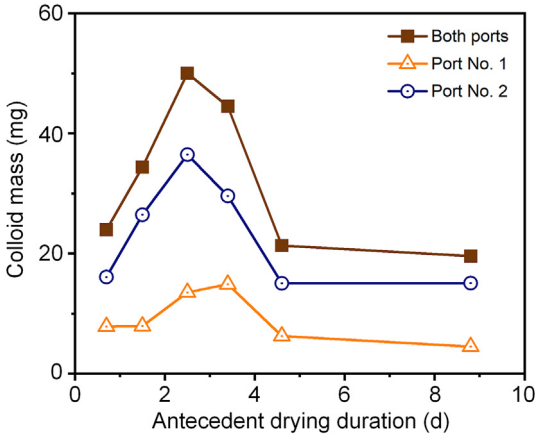

Fig. 2. Effect of antecedent drying duration on the total mass of colloids mobilized through the active ports during dry–wet cycles.

Table 1
BDE-209 concentration in the effluents from soil cores under different hydrodynamic conditions.

Hydrodynamic condition	Range (ng/L)	Mean ± SD (ng/L)
Dry–wet cycles	ND–0.48	0.21 ± 0.15
Freeze–thaw cycles	0.08–0.34	0.19 ± 0.09

BDE-209, 2,2′,3,3′,4,4′,5,5′,6,6′-decabromodiphenyl ether; ND, below the method detection limit (0.07 ng/L); SD, standard deviation.

3.2. Effects of freeze–thaw cycles on the release of colloids and BDE-209

In the freeze–thaw leaching experiments, water also eluted from only two of the seven ports (Fig. 3). Compared to the dry–wet cycles, the freeze–thaw cycles led to an increase in the released colloidal concentration (Fig. 3 and Table S4). During each freeze–thaw leaching cycle, peak colloidal concentrations (as high as 76 mg/L) were observed in the effluent collected within the first 12 h, which then gradually decreased. This high initial colloid release was primarily attributed to the volumetric expansion of water during the freezing process, exerting mechanical stress on the pore walls, which disintegrates soil aggregates and promotes colloid formation [50,61–64]. The average D_h of colloids in the effluent ranged from 317 ± 25 to 360 ± 16 nm (Fig. 3 and Table S4), lower than that eluted during the dry–wet cycles (Fig. 1 and Table S3), suggesting greater extents of disintegration of soil aggregates during freeze–thaw cycles. The ζ-potential of colloids in the effluent was relatively stable during each freeze–thaw cycle test, but in the first cycle, the ζ-potential was more negative than in other cycles, possibly due to the elution of microbially derived organic substances, as indicated from the excitation/emission peak at 300/375 nm in the EEM spectrum (Fig. S3a) [65,66]. By contrast, in the following four cycles, the effluent only contained low levels of protein-like substances, as indicated by the excitation/emission peak at 220/300 nm in the EEM spectra (Fig. S3b–e) [65,67,68].

The freeze–thaw cycles appeared to exert negligible influence on the conductivity of the effluent (Fig. 3). During each leaching test, the conductivity declined over time, from 91.6–127.0 μS/cm (on average 110.4 ± 10.4 μS/cm) to 66.9–73.0 μS/cm (on average 70.3 ± 2.2 μS/cm). The relatively low conductivity corresponds to the lower ionic strength of the effluent, which may contribute to the smaller D_h and slightly more negative ζ-potential of the colloids eluted from the freeze–thaw cycle tests. Moreover, the effluent pH remained stable between 7.5 and 7.7 also because of the pH buffering capacity of the soil.

During the freeze–thaw leaching experiments, BDE-209 concentrations in all of the effluent samples were above the MDL of 0.07 ng/L, with values ranging from 0.08 to 0.34 ng/L and, on average, 0.19 ± 0.09 ng/L (Table 1 and Table S4). Notably, compared with the dry–wet cycles, although the freeze–thaw cycles enhanced colloid release, the BDE-209 concentrations in the effluent were not significantly different between the two sets of experiments (Table 1). This result appears to contradict the predictions from the colloid-facilitated release of contaminants. However, further analysis shows that colloid-facilitated release still plays a key role in the release of BDE-209 from the soil under different transient flow conditions, as discussed in the following.

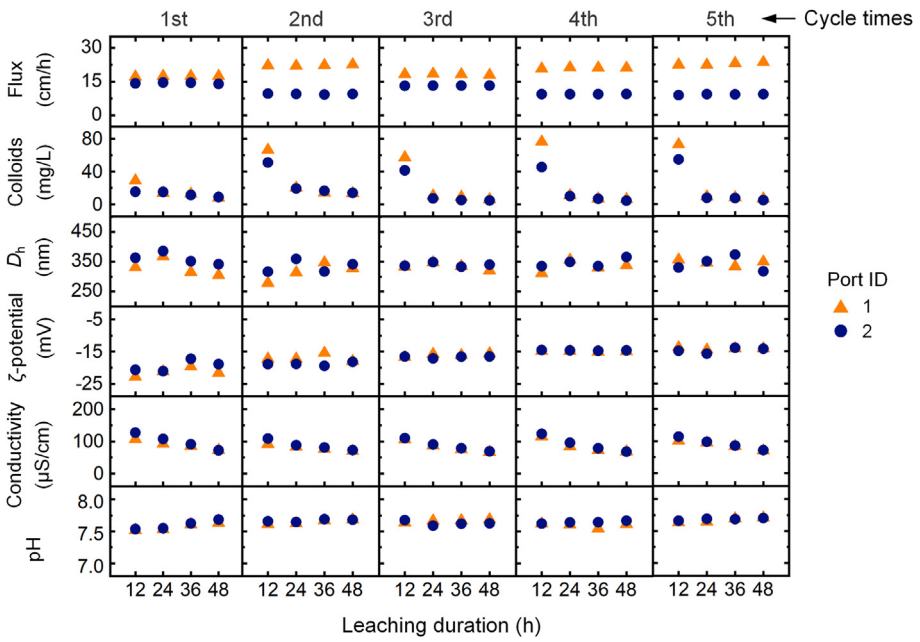

Fig. 3. Effluent flux, colloid concentration, D_h, ζ-potential, conductivity, and pH at two active ports during freeze–thaw cycle tests. Influent Darcy velocity = 1.5 cm/h, ionic strength = 0.01 mM, pH = 4.4.

3.3. *Mechanisms for differential effects of dry–wet and freeze–thaw cycles on colloid-facilitated release of BDE-209*

It has long been recognized that soil colloids play a key role in facilitating the release and subsurface migration of hydrophobic organic pollutants, such as polycyclic aromatic hydrocarbons [69–71], atrazine [72,73], bismerthiazol [74], polychlorinated biphenyls [75], and PBDEs [38,40,76,77]. Consistent with the previous findings, in this study, we observed significant positive correlations ($p < 0.01$) between the concentrations of colloids and BDE-209 in leachates from soil cores in either the dry–wet or the freeze–thaw cycle tests (Fig. 4), although when data from both sets of cycle tests were pooled together, there was no significant correlation ($p = 0.05$). Notably, due to the hydrophobicity and extremely low solubility of BDE-209, the slope of the regression curve can, to some extent, indicate the content of BDE-209 bound to colloids in the effluent. The slope of the regression curve for the dry–wet cycle tests was higher than that for the freeze–thaw cycle tests (Fig. 4), suggesting that the colloids eluted during the dry–wet cycle tests had higher BDE-209 content than those eluted during the freeze–thaw cycle tests.

The mechanisms for the differential effects of dry–wet and freeze–thaw cycles on the colloid-facilitated release of BDE-209 were examined by characterizing the physicochemical properties of the eluted colloids. Organic carbon can enhance the capability of soil colloids to bind PBDEs [40,41], and different organic contents in the eluted colloids between the dry–wet and freeze–thaw cycles may contribute to the different BDE-209 contents in the colloids. The small amount of colloids in the effluent precludes the quantitative analysis of their organic carbon contents by elemental analysis. However, according to the EEM spectra (Fig. S4), the effluent in the dry–wet cycle tests contained microbially derived and protein-like organic substances at concentrations higher than those in the freeze–thaw cycle tests (except the first cycle). Nevertheless, the effluent sampled from the first cycle of the freeze–thaw cycle tests contained relatively low BDE-209 concentrations (Table S4), despite the abundance of organic matter (Fig. S3). Therefore, other factors likely have led to the differential effects of the dry–wet and freeze–thaw cycles. As mentioned in *Section* 3.2, the effluent in the freeze–thaw cycle tests contained higher colloid concentrations than that in the dry–wet cycle tests. Moreover, the second to fifth cycles of the freeze–thaw cycle tests yielded higher colloid concentrations than did the first cycle (Fig. 3), despite the much lower organic matter abundance in the effluents (Fig. S3). Therefore, it can be inferred that the freeze–thaw cycles induced the release of more inorganic colloidal components, and it is hypothesized that these inorganic colloids contained low contents of BDE-209, which diluted the overall BDE-209 content in the eluted colloids.

According to XRD characterization results (Fig. 5), the major mineral components of colloids in the effluent from the dry–wet cycle tests were calcite ($CaCO_3$), whereas in the freeze–thaw cycles, the eluted colloids were mainly composed of $CaCO_3$, quartz (SiO_2), and albite ($NaAlSi_3O_8$). Note that clay minerals are also important components of soil colloids [50], though their characteristic peaks were not observed in the XRD patterns, possibly due to their low crystallinity in the effluents as well as due to the incomplete separation of nanoscale clay particles during the centrifugation (at 1617×*g* for 25 min). It has been

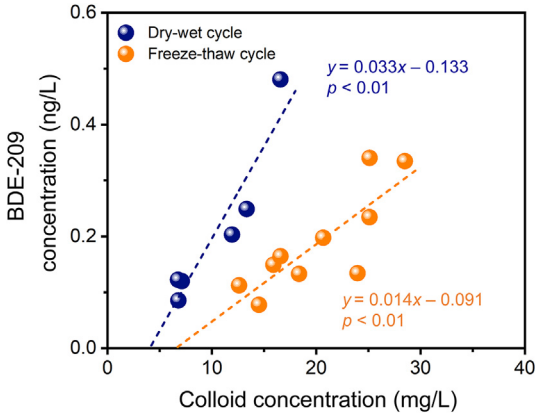

Fig. 4. Correlation between colloid and BDE-209 concentrations in the effluent from soil cores, measured in dry–wet and freeze–thaw leaching tests. The dashed lines represent the regression curves.

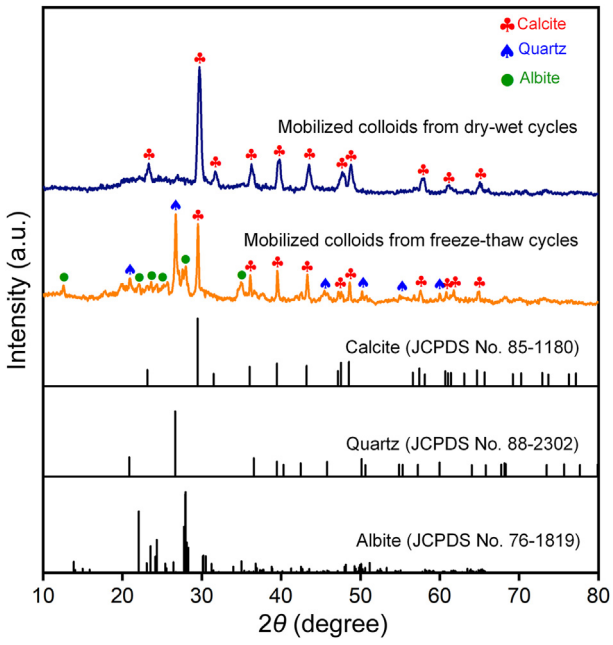

Fig. 5. X-ray diffraction patterns of mobilized colloids from dry–wet cycles and freeze–thaw cycles.

reported that the capillary stress during dry–wet cycles may not mobilize quartz colloids, whereas the mechanical stress during the freeze–thaw processes could break bulk particles of quartz and possibly other primary silicate minerals (e.g., albite) to form the corresponding colloidal particles [50,53,78]. Indeed, TEM analysis (Fig. S5) revealed that particles with smoother surfaces were observed in the effluent from the freeze–thaw leaching experiments, which were likely the colloidal particles formed via the breaking of bulk minerals and exhibiting smooth cleavage planes. These newly formed inorganic colloidal fractions were supposed to contain lower contents of BDE-209, contributing to the different slopes of the regression curves in Fig. 4. Notably, the intercept of the regression curves on the abscissa was higher for the freeze–thaw cycle tests than for the dry–wet cycle tests (Fig. 4), further substantiating the hypothesis that the colloids eluted from the freeze–thaw cycle tests contained higher fractions of particles with extremely low BDE-209 content.

4. Conclusion

Leaching experiments using undisturbed soil cores under dry–wet and freeze–thaw cycle conditions showed significant positive correlations between concentrations of colloids and BDE-209 in the leachate. However, colloids mobilized during the dry–wet cycles contained higher contents of BDE-209 than those in the freeze–thaw cycle tests. These results demonstrate the critical role of soil colloids in facilitating BDE-209 release and downward migration in the subsurface, which varies under different transient flow conditions. The differences can be attributed to varying degrees of alteration in soil structure under these conditions, leading to distinct colloid types. During dry–wet cycles, the drying process lowers soil moisture and induces capillary stress, breaking down soil pore walls and generating colloids with more BDE-209. Conversely, during freeze–thaw cycles, the mechanical stress due to the expansion and contraction of water and ice disrupts soil aggregates more intensely, forming inorganic colloidal particles (mainly primary silicate minerals such as quartz and albite) with low BDE-209 content. These results underscore the significance of transient flow conditions in altering the mobility of PBDEs in the subsurface, emphasizing the necessity of considering these conditions when predicting the fate and risks of PBDEs at contaminated sites. Furthermore, these findings can aid in the design of hydrological intervention measures to curtail the colloid-facilitated spreading of hydrophobic POPs into sensitive subsurface environments, so as to mitigate human exposure to these hazardous substances through groundwater.

CRediT authorship contribution statement

Y.Y.L. and Z.B.H.: data curation, investigation, visualization, writing—original draft. Y.Q.Y.: investigation. L.D.: writing—review and editing. C.J.J.: conceptualization, funding acquisition, investigation, supervision, writing—original draft, writing—review and editing. W.C.: funding acquisition, supervision, writing—review and editing.

Declaration of competing interests

There are no conflicts of interest to declare.

Acknowledgments

This work was supported by the National Key Research and Development Program of China (2019YFC1804202), the National Natural Science Foundation of China (22276101 and 22020102004), the Fundamental Research Funds for the Central Universities (63233056), and the Ministry of Education of China (T2017002).

Appendix A. Supplementary data

Supplementary data to this article can be found online at https://doi.org/10.1016/j.eehl.2024.03.002.

References

[1] M. Alaee, An overview of commercially used brominated flame retardants, their applications, their use patterns in different countries/regions and possible modes of release, Environ. Int. 29 (2003) 683–689, https://doi.org/10.1016/S0160-4120(03)00121-1.
[2] P. De Oro-Carretero, J. Sanz-Landaluze, Bioaccumulation and biotransformation of BDE-47 using zebrafish eleutheroembryos (*Danio rerio*), Environ. Toxicol. Chem. 42 (2023) 835–845, https://doi.org/10.1002/etc.5569.
[3] A. Zandona, K. Jagic, M. Dvorscak, J. Madunic, D. Klincic, M. Katalinic, PBDEs found in house dust impact human lung epithelial cell homeostasis, Toxics 10 (2022) 97, https://doi.org/10.3390/toxics10020097.
[4] H.A. Leslie, P.E.G. Leonards, S.H. Brandsma, J. De Boer, N. Jonkers, Propelling plastics into the circular economy-weeding out the toxics first, Environ. Int. 94 (2016) 230–234, https://doi.org/10.1016/j.envint.2016.05.012.
[5] M. Sharkey, S. Harrad, M. Abou-Elwafa Abdallah, D.S. Drage, H. Berresheim, Phasing-out of legacy brominated flame retardants: the UNEP Stockholm Convention and other legislative action worldwide, Environ. Int. 144 (2020) 106041, https://doi.org/10.1016/j.envint.2020.106041.
[6] H. Lilienthal, A. Hack, A. Roth-Härer, S.W. Grande, C.E. Talsness, Effects of developmental exposure to 2,2',4,4',5-pentabromodiphenyl ether (PBDE-99) on sex steroids, sexual development, and sexually dimorphic behavior in rats, Environ. Health Perspect. 114 (2006) 194–201, https://doi.org/10.1289/ehp.8391.
[7] A. Konstantinov, B. Chittim, D. Potter, J. Klein, N. Riddell, R. McCrindle, Is BDE-175 an important enough component of commercial octabromodiphenyl ether mixtures to be listed in Annex A of the Stockholm Convention? Chemosphere 82 (2011) 778–781, https://doi.org/10.1016/j.chemosphere.2010.11.016.
[8] J.O. Babayemi, O. Osibanjo, O. Sindiku, R. Weber, Inventory and substance flow analysis of polybrominated diphenyl ethers in the Nigerian transport sector—end-of-life vehicles policy and management, Environ. Sci. Pollut. Res. 25 (2016) 31805–31818, https://doi.org/10.1007/s11356-016-6574-8.
[9] United Nations Environment Programme, All POPs listed in the Stockholm Convention. 2019. https://chm.pops.int/TheConvention/ThePOPs/AllPOPs/tabid/2509/Default.aspx. (Accessed 27 February 2024).
[10] M. Garcia Lopez, M. Driffield, A.R. Fernandes, F. Smith, J. Tarbin, A.S. Lloyd, et al., Occurrence of polybrominated diphenylethers, hexabromocyclododecanes, bromophenols and tetrabromobisphenols A and S in Irish foods, Chemosphere 197 (2018) 709–715, https://doi.org/10.1016/j.chemosphere.2018.01.089.
[11] S. Ma, G. Ren, K. Zheng, J. Cui, P. Li, X. Huang, et al., New insights into human biotransformation of BDE-209: unique occurrence of metabolites of ortho-substituted hydroxylated higher brominated diphenyl ethers in the serum of e-waste dismantlers, Environ. Sci. Technol. 56 (2022) 10239–10248, https://doi.org/10.1021/acs.est.2c02074.
[12] M.Y. Zou, Y. Ran, J. Gong, B.X. Maw, E.Y. Zeng, Polybrominated diphenyl ethers in watershed soils of the Pearl River Delta, China: occurrence, inventory, and fate, Environ. Sci. Technol. 41 (2007) 8262–8267, https://doi.org/10.1021/es071956d.

[13] A.O.W. Leung, W.J. Luksemburg, A.S. Wong, M.H. Wong, Spatial distribution of polybrominated diphenyl ethers and polychlorinated dibenzo-p-dioxins and dibenzofurans in soil and combusted residue at Guiyu, an electronic waste recycling site in southeast China, Environ. Sci. Technol. 41 (2007) 2730–2737, https://doi.org/10.1021/es0625935.
[14] W.L. Li, W.L. Ma, H.L. Jia, W.J. Hong, H.B. Moon, H. Nakata, et al., Polybrominated diphenyl ethers (PBDEs) in surface soils across five Asian countries: levels, spatial distribution, and source contribution, Environ. Sci. Technol. 50 (2016) 12779–12788, https://doi.org/10.1021/acs.est.6b04046.
[15] Z. Wu, W. Han, M. Xie, M. Han, Y. Li, Y. Wang, Occurrence and distribution of polybrominated diphenyl ethers in soils from an e-waste recycling area in northern China, Ecotoxicol. Environ. Saf. 167 (2019) 467–475, https://doi.org/10.1016/j.ecoenv.2018.10.029.
[16] I. Labunsk, S. Harrad, D. Santillo, P. Johnston, K. Brigden, Levels and distribution of polybrominated diphenyl ethers in soil, sediment and dust samples collected from various electronic waste recycling sites within Guiyu town, southern China, Environ. Sci.: Processes Impacts 15 (2013) 503–511, https://doi.org/10.1039/c2em30785e.
[17] J.X. Wang, L.L. Liu, J.F. Wang, B.S. Pan, X.X. Fu, G. Zhang, et al., Distribution of metals and brominated flame retardants (BFRs) in sediments, soils and plants from an informal e-waste dismantling site, South China, Environ. Sci. Pollut. Res. 22 (2015) 1020–1033, https://doi.org/10.1007/s11356-014-3399-1.
[18] B.X. Mai, S.J. Chen, X.J. Luo, L.G. Chen, Q.S. Yang, G.Y. Sheng, et al., Distribution of polybrominated diphenyl ethers in sediments of the Pearl River Delta and adjacent South China Sea, Environ. Sci. Technol. 39 (2005) 3521–3527, https://doi.org/10.1021/es048083x.
[19] M.J. He, X.J. Luo, M.Y. Chen, Y.X. Sun, S.J. Chen, B.X. Mai, Bioaccumulation of polybrominated diphenyl ethers and decabromodiphenyl ethane in fish from a river system in a highly industrialized area, South China, Sci. Total Environ. 419 (2012) 109–115, https://doi.org/10.1016/j.scitotenv.2011.12.035.
[20] X.F. Zhu, Y. Zhong, H.L. Wang, D. Li, Y.R. Deng, P.A. Peng, New insights into the anaerobic microbial degradation of decabrominated diphenyl ether (BDE-209) in coastal marine sediments, Environ. Pollut. 255 (2019) 113151, https://doi.org/10.1016/j.envpol.2019.113151.
[21] Y. Kang, H.S. Wang, K.C. Cheung, M.H. Wong, Polybrominated diphenyl ethers (PBDEs) in indoor dust and human hair, Atmos. Environ. 45 (2011) 2386–2393, https://doi.org/10.1016/j.atmosenv.2011.02.019.
[22] A. Besis, C. Samara, Polybrominated diphenyl ethers (PBDEs) in the indoor and outdoor environments - a review on occurrence and human exposure, Environ. Pollut. 169 (2012) 217–229, https://doi.org/10.1016/j.envpol.2012.04.009.
[23] X.B. Zheng, L. Qiao, A. Covaci, R.X. Sun, H.Y. Guo, J. Zheng, et al., Brominated and phosphate flame retardants (FRs) in indoor dust from different microenvironments: implications for human exposure via dust ingestion and dermal contact, Chemosphere 184 (2017) 185–191, https://doi.org/10.1016/j.chemosphere.2017.05.167.
[24] J. Muñoz-Arnanz, M. Sáez, J.I. Aguirre, F. Hiraldo, R. Baos, G. Pacepavicius, et al., Predominance of BDE-209 and other higher brominated diphenyl ethers in eggs of white stork (*Ciconia ciconia*) colonies from Spain, Environ. Int. 37 (2011) 572–576, https://doi.org/10.1016/j.envint.2010.11.013.
[25] R. Sutton, M.D. Sedlak, D. Yee, J.A. Davis, D. Crane, R. Grace, et al., Declines in polybrominated diphenyl ether contamination of San Francisco Bay following production phase-outs and bans, Environ. Sci. Technol. 49 (2015) 777–784, https://doi.org/10.1021/es503727b.
[26] Ministry of Ecology and Environment of the People's Republic of China, List of new pollutants under control. https://www.gov.cn/zhengce/2022-12/30/content_5734728.htm, 2023. (Accessed 27 February 2024).
[27] R.J. Law, A. Covaci, S. Harrad, D. Herzke, M.A.-E. Abdallah, K. Fernie, et al., Levels and trends of PBDEs and HBCDs in the global environment: status at the end of 2012, Environ. Int. 65 (2014) 147–158, https://doi.org/10.1016/j.envint.2014.01.006.
[28] J.J. Kim, K. Delisle, T.M. Brown, F. Bishay, P.S. Ross, M. Noël, Characterization and interpolation of sediment polychlorinated biphenyls and polybrominated diphenyl ethers in resident killer whale habitat along the coast of British Columbia, Canada, Environ. Toxicol. Chem. 41 (2022) 2139–2151, https://doi.org/10.1002/etc.5404.
[29] D. Chen, X. Bi, J. Zhao, L. Chen, J. Tan, B. Mai, et al., Pollution characterization and diurnal variation of PBDEs in the atmosphere of an E-waste dismantling region, Environ. Pollut. 157 (2009) 1051–1057, https://doi.org/10.1016/j.envpol.2008.06.005.
[30] S. Gao, J. Hong, Z. Yu, J. Wang, G. Yang, G. Sheng, et al., Polybrominated diphenyl ethers in surface soils from e-waste recycling areas and industrial areas in South China: concentration levels, congener profile, and inventory, Environ. Toxicol. Chem. 30 (2011) 2688–2696, https://doi.org/10.1002/etc.668.
[31] A. Kerric, J. Okeme, L. Jantunen, J.-F. Giroux, M.L. Diamond, J. Verreault, Spatial and temporal variations of halogenated flame retardants and organophosphate esters in landfill air: potential linkages with gull exposure, Environ. Pollut. 271 (2021) 116396, https://doi.org/10.1016/j.envpol.2020.116396.
[32] I. Navarro, A. De La Torre, P. Sanz, M.Á. Porcel, G. Carbonell, M.D.L.Á. Martínez, Transfer of perfluorooctanesulfonate (PFOS), decabrominated diphenyl ether (BDE-209) and Dechlorane Plus (DP) from biosolid-amended soils to leachate and runoff water, Environ. Chem. 15 (2018) 195–204, https://doi.org/10.1071/EN18032.
[33] J. Levison, K. Novakowski, E.J. Reiner, T. Kolic, Potential of groundwater contamination by polybrominated diphenyl ethers (PBDEs) in a sensitive bedrock aquifer (Canada), Hydrogeol. J. 20 (2012) 401–412, https://doi.org/10.1007/s10040-011-0813-3.
[34] N. Gottschall, E. Topp, M. Edwards, M. Payne, S. Kleywegt, D.R. Lapen, Brominated flame retardants and perfluoroalkyl acids in groundwater, tile drainage, soil, and crop grain following a high application of municipal biosolids to a field, Sci. Total Environ. 574 (2017) 1345–1359, https://doi.org/10.1016/j.scitotenv.2016.08.044.
[35] Y. Zhang, B. Xi, W. Tan, Release, transformation, and risk factors of polybrominated diphenyl ethers from landfills to the surrounding environments: a review, Environ. Int. 157 (2021) 106780, https://doi.org/10.1016/j.envint.2021.106780.
[36] L.W. de Jonge, C. Kjaergaard, P. Moldrup, Colloids and colloid-facilitated transport of contaminants in soils: an introduction, Vadose Zone J. 3 (2004) 321–325, https://doi.org/10.2136/vzj2004.0321.
[37] T. Kanti Sen, K.C. Khilar, Review on subsurface colloids and colloid-associated contaminant transport in saturated porous media, Adv. Colloid Interface Sci. 119 (2006) 71–96, https://doi.org/10.1016/j.cis.2005.09.001.
[38] Z. Huo, M. Xi, L. Xu, C. Jiang, Colloid-facilitated release of polybrominated diphenyl ethers at an e-waste recycling site: evidence from undisturbed soil core leaching experiments, Front. Environ. Sci. Eng. 18 (2024) 21, https://doi.org/10.1007/s11783-024-1781-x.
[39] M. Flury, H. Qiu, Modeling colloid-facilitated contaminant transport in the vadose zone, Vadose Zone J. 7 (2008) 682–697, https://doi.org/10.2136/vzj2007.0066.
[40] S. Yu, P. Zou, W. Zhu, L. Xiao, A.J. Miao, L.J. Jiang, et al., Effects of humic acid and Tween-80 on behavior of decabromodiphenyl ether in soil columns, Environ. Earth Sci. 69 (2013) 1523–1528, https://doi.org/10.1007/s12665-012-1986-3.
[41] L. Duan, Y. Ying, J. Zhong, C. Jiang, W. Chen, Key factors controlling colloids–bulk soil distribution of polybrominated diphenyl ethers (PBDEs) at an e-waste recycling site: implications for PBDE mobility in subsurface environment, Sci. Total Environ. 819 (2022) 153080, https://doi.org/10.1016/j.scitotenv.2022.153080.
[42] J.E. Saiers, J.J. Lenhart, Colloid mobilization and transport within unsaturated porous media under transient-flow conditions, Water Resour. Res. 39 (2003) 1019, https://doi.org/10.1029/2002wr001370.
[43] J.Y. Shang, M. Flury, G. Chen, J. Zhuang, Impact of flow rate, water content, and capillary forces on in situ colloid mobilization during infiltration in unsaturated sediments, Water Resour. Res. 44 (2008) W06411, https://doi.org/10.1029/2007wr006516.
[44] Y.H. El-Farhan, N.M. DeNovio, J.S. Herman, G.M. Hornberger, Mobilization and transport of soil particles during infiltration experiments in an agricultural field, Shenandoah Valley, Virginia, Environ. Sci. Technol. 34 (2000) 3555–3559, https://doi.org/10.1021/es991099g.
[45] T. Cheng, J.E. Saiers, Colloid-facilitated transport of cesium in vadose-zone sediments: the importance of flow transients, Environ. Sci. Technol. 44 (2010) 7443–7449, https://doi.org/10.1021/es100391j.
[46] C. Wang, C.P. McNew, S.W. Lyon, M.T. Walter, T.H.M. Volkman, N. Abramson, et al., Particle tracer transport in a sloping soil lysimeter under periodic, steady state conditions, J. Hydrol. 569 (2019) 61–76, https://doi.org/10.1016/j.jhydrol.2018.11.050.
[47] J. Zhuang, J.F. McCarthy, J.S. Tyner, E. Perfect, M. Flury, In situ colloid mobilization in Hanford sediments under unsaturated transient flow conditions: effect of irrigation pattern, Environ. Sci. Technol. 41 (2007) 3199–3204, https://doi.org/10.1021/es062757h.
[48] S.K. Mohanty, J.E. Saiers, J.N. Ryan, Colloid mobilization in a fractured soil during dry–wet cycles: role of drying duration and flow path permeability, Environ. Sci. Technol. 49 (2015) 9100–9106, https://doi.org/10.1021/acs.est.5b00889.
[49] L. Chequer, P. Bedrikovetsky, T. Carageorgos, A. Badalyan, V. Gitis, Mobilization of attached clustered colloids in porous media, Water Resour. Res. 55 (2019) 5696–5714, https://doi.org/10.1029/2018WR024504.
[50] S.K. Mohanty, J.E. Saiers, J.N. Ryan, Colloid-facilitated mobilization of metals by freeze-thaw cycles, Environ. Sci. Technol. 48 (2014) 977–984, https://doi.org/10.1021/es403698u.
[51] B. Gao, J.E. Saiers, J. Ryan, Pore-scale mechanisms of colloid deposition and mobilization during steady and transient flow through unsaturated granular media, Water Resour. Res. 42 (2006) W01410, https://doi.org/10.1029/2005wr004233.
[52] S. Majdalani, E. Michel, L. Di-Pietro, R. Angulo-Jaramillo, Effects of wetting and drying cycles on *in situ* soil particle mobilization, Eur. J. Soil Sci. 59 (2008) 147–155, https://doi.org/10.1111/j.1365-2389.2007.00964.x.
[53] N.W. Hu, H.W. Yu, Q.R. Wang, G.P. Zhu, X.T. Yang, T.Y. Wang, et al., Colloid-facilitated mobilization of cadmium: comparison of spring freeze-thaw event and autumn freeze-thaw event, Sci. Total Environ. 852 (2022) 158467, https://doi.org/10.1016/j.scitotenv.2022.158467.
[54] S.K. Mohanty, J.E. Saiers, J.N. Ryan, Colloid mobilization in a fractured soil: effect of pore-water exchange between preferential flow paths and soil matrix, Environ. Sci. Technol. 50 (2016) 2310–2317, https://doi.org/10.1021/acs.est.5b04767.
[55] T.L. Ter Laak, F.J.M. Busser, J.L.M. Hermens, Poly(dimethylsiloxane) as passive sampler material for hydrophobic chemicals: effect of chemical properties and sampler characteristics on partitioning and equilibration times, Anal. Chem. 80 (2008) 3859–3866, https://doi.org/10.1021/ac800258j.
[56] P. Lehmann, D. Or, Evaporation and capillary coupling across vertical textural contrasts in porous media, Phys. Rev. E 80 (2009) 046318, https://doi.org/10.1103/PhysRevE.80.046318.
[57] C. Lu, Y.G. Wu, S. Hu, Drying-wetting cycles facilitated mobilization and transport of metal-rich colloidal particles from exposed mine tailing into soil in a gold mining region along the Silk Road, Environ. Earth Sci. 75 (2016) 1031, https://doi.org/10.1007/s12665-016-5812-1.
[58] E. Michel, S. Majdalani, L. Di-Pietro, How differential capillary stresses promote particle mobilization in macroporous soils: a novel conceptual model, Vadose Zone J. 9 (2010) 307–316, https://doi.org/10.2136/vzj2009.0084.

[59] P.M. Jardine, G.K. Jacobs, G.V. Wilson, Unsaturated transport processes in undisturbed heterogeneous porous media: I. Inorganic contaminants, Soil Sci. Soc. Am. J. 57 (1993) 945–953, https://doi.org/10.2136/sssaj1993.03615995005700040012x.
[60] S. Sirivithayapakorn, A. Keller, Transport of colloids in unsaturated porous media: a pore-scale observation of processes during the dissolution of air-water interface, Water Resour. Res. 39 (2003) 1346, https://doi.org/10.1029/2003WR002487.
[61] M. Xu, Y. Zheng, W. Chen, N. Mao, P. Guo, Leachate properties and cadmium migration through freeze-thaw treated soil columns, Bull. Environ. Contam. Toxicol. 98 (2017) 113–119, https://doi.org/10.1007/s00128-016-1982-5.
[62] T. Oztas, F. Fayetorbay, Effect of freezing and thawing processes on soil aggregate stability, CATENA 52 (2003) 1–8, https://doi.org/10.1016/S0341-8162(02)00177-7.
[63] S.H. Kværnø, L. Øygarden, The influence of freeze–thaw cycles and soil moisture on aggregate stability of three soils in Norway, CATENA 67 (2006) 175–182, https://doi.org/10.1016/j.catena.2006.03.011.
[64] Z. Wang, Y.L. Zhang, M. Flury, H.T. Zou, Freeze-thaw cycles lead to enhanced colloid-facilitated Pb transport in a Chernozem soil, J. Contam. Hydrol. 251 (2022) 104093, https://doi.org/10.1016/j.jconhyd.2022.104093.
[65] W. Chen, P. Westerhoff, J.A. Leenheer, K. Booksh, Fluorescence excitation - emission matrix regional integration to quantify spectra for dissolved organic matter, Environ. Sci. Technol. 37 (2003) 5701–5710, https://doi.org/10.1021/es034354c.
[66] Y. Yamashita, R. Jaffé, Characterizing the interactions between trace metals and dissolved organic matter using excitation-emission matrix and parallel factor analysis, Environ. Sci. Technol. 42 (2008) 7374–7379, https://doi.org/10.1021/es801357h.
[67] N. Hudson, A. Baker, D. Reynolds, Fluorescence analysis of dissolved organic matter in natural, waste and polluted waters - a review, River Res. Appl. 23 (2007) 631–649, https://doi.org/10.1002/rra.1005.
[68] A. Dubnick, J. Barker, M. Sharp, J. Wadham, G. Lis, J. Telling, et al., Characterization of dissolved organic matter (DOM) from glacial environments using total fluorescence spectroscopy and parallel factor analysis, Ann. Glaciol. 51 (2010) 111–122, https://doi.org/10.3189/172756411795931912.
[69] S.B. Roy, D.A. Dzombak, Chemical factors influencing colloid-facilitated transport of contaminants in porous media, Environ. Sci. Technol. 31 (1997) 656–664, https://doi.org/10.1021/es9600643.
[70] K.U. Totsche, S. Jann, I. Kögel-Knabner, Single event-driven export of polycyclic aromatic hydrocarbons and suspended matter from coal tar-contaminated soil, Vadose Zone J. 6 (2007) 233–243, https://doi.org/10.2136/vzj2006.0083.
[71] F. Liu, B.L. Xu, Y. He, P.C. Brookes, J.M. Xu, Co-transport of phenanthrene and pentachlorophenol by natural soil nanoparticles through saturated sand columns, Environ. Pollut. 249 (2019) 406–413, https://doi.org/10.1016/j.envpol.2019.03.052.
[72] L.A. Sprague, J.S. Herman, G.M. Hornberger, A.L. Mills, Atrazine adsorption and colloid-facilitated transport through the unsaturated zone, J. Environ. Qual. 29 (2000) 1632–1641, https://doi.org/10.2134/jeq2000.00472425002900050034x.
[73] A.K. Seta, A.D. Karathanasis, Atrazine adsorption by soil colloids and co-transport through subsurface environments, Soil Sci. Soc. Am. J. 61 (1997) 612–617, https://doi.org/10.2136/sssaj1997.03615995006100020034x.
[74] C.Y. Shen, H. Wang, V. Lazouskaya, Y.C. Du, W.L. Lu, J.X. Wu, et al., Cotransport of bismerthiazol and montmorillonite colloids in saturated porous media, J. Contam. Hydrol. 177 (2015) 18–29, https://doi.org/10.1016/j.jconhyd.2015.03.003.
[75] D.G. Chatzikosma, E.A. Voudrias, Simulation of polychlorinated biphenyls transport in the vadose zone, Environ. Geol. 53 (2007) 211–220, https://doi.org/10.1007/s00254-006-0635-0.
[76] T. Gorgy, L.Y. Li, J.R. Grace, M.G. Ikonomou, Polybrominated diphenyl ethers mobility in biosolids-amended soils using leaching column tests, Water Air Soil Pollut. 222 (2011) 77–90, https://doi.org/10.1007/s11270-011-0810-0.
[77] W.K. Qiu, T. Ma, R. Liu, Y. Du, Aluminum hydroxide colloid facilitated transport of 2,2',4,4'-tetrabromodiphenyl ether (BDE-47) in porous media, Chemosphere 258 (2020) 127321, https://doi.org/10.1016/j.chemosphere.2020.127321.
[78] G.A. Lehrsch, R.E. Sojka, D.L. Carter, P.M. Jolley, Freezing effects on aggregate stability affected by texture, mineralogy, and organic matter, Soil Sci. Soc. Am. J. 55 (1991) 1401–1406, https://doi.org/10.2136/sssaj1991.03615995005500050033x.